

INTERNATIONAL CENTRE FOR THEORETICAL PHYSICS

A MICROSCOPIC STUDY OF THE S BAND
IN THE GENERATOR CO-ORDINATE APPROACH

E. Wüst

and

A. Ansari



**INTERNATIONAL
ATOMIC ENERGY
AGENCY**



**UNITED NATIONS
EDUCATIONAL,
SCIENTIFIC
AND CULTURAL
ORGANIZATION**

1985 MIRAMARE-TRIESTE



International Atomic Energy Agency
and
United Nations Educational Scientific and Cultural Organization

INTERNATIONAL CENTRE FOR THEORETICAL PHYSICS

A MICROSCOPIC STUDY OF THE S BAND
IN THE GENERATOR CO-ORDINATE APPROACH *

E. Wüst
Department of Physics, SUNY, Stony Brook, N.Y., USA,

and

A. Ansari **
International Centre for Theoretical Physics, Trieste, Italy.

ABSTRACT

Using particle number and spin projected cranked Hartree-Fock-Bogolubov (CHFb) wave functions in the generator co-ordinate method (GCM) with the cranking frequency as a GC the shortcomings of the usual CHFb theory are removed and the ground as well as the s band are studied simultaneously. In particular, low-spin properties of the s band are discussed for a backbending nucleus ^{158}Dy .

MIRAMARE - TRIESTE

April 1985

* To be submitted for publication.

** Permanent address: Institute of Physics, Bhubaneswar-751005, India.

A few years back Alberger et al.[1] had suggested how to populate the spin-aligned non-yrast low-spin levels of the s band in light ion reactions like ($^3\text{He},\alpha$) on even-odd rare-earth nuclei for which the odd neutron is in the $i_{13/2}$ orbitals. They have discussed these in great detail (e.g. Fig.2 in Ref.1) particularly for a ^{161}Dy target.

Recently, we have studied some properties of the low-spin members of the s band for a backbending nucleus ^{158}Dy [2] following the number and spin projected [3,4] CHFb approach [5,6]. In Ref.2 (hereafter referred to as I) the orthogonality of a low spin g-band state to the same spin s-band state was not guaranteed due to the lack of computer time, though due to their non-aligned and aligned structure the mutual overlap at a given I was expected to be small. There we had checked for the effect of mixing of $|\omega_{12}\rangle$ and $|\omega_{14}\rangle$ CHFb wave functions through a generator co-ordinate method (GCM) calculation. The state $|\omega_I\rangle$ indicates a self-consistent CHFb solution with a cranking frequency ω_I satisfying the angular momentum constraint

$$\langle \psi(\omega_I) | J_x | \psi(\omega_I) \rangle = I_x = \sqrt{I(I+1)} \quad (1)$$

along with the usual particle number constraints [5,6].

This note is essentially a continuation of I. Here through a discretized GCM approach [7-9] treating ω ($\omega_0, \omega_2, \dots, \omega_{16}$) as a GC the physical wave function is defined by

$$\psi_I = \sum_i f_i(\omega_i) \psi_I(\omega_i) \quad , \quad (2)$$

where $\psi_I(\omega_i)$ is a number and spin projected CHFb wave function, and f_i is the weight factor. Then the Hill-Wheeler eigenvalue equation [7-9]

$$H_I f_I = E_I N_I f_I \quad (3)$$

is solved, H and N being the Hamiltonian and overlap kernels. Technical details regarding the solution of Eq.(3) are very well discussed by Ring and Schuck [9]. The first essential step is to diagonalize N_I and we want to mention that we have ignored the eigenvalues n_i which satisfy the condition $n_i/n_1 < 10^{-2}$, where n_1 is the largest eigenvalue. Also we must point out, as emphasized in Ref.4, that a number projection is essential in such a GCM calculation.

We present in Table I the overlaps $\langle \omega_0 | \omega_I \rangle$ to have an idea how well the g band and the aligned s band can mix. Of particular interest is the last column for $\langle \omega_0 | \omega_{16} \rangle$ and these numbers are rather small even for I in the band crossing region. Of course, for the intermediate states the overlap is large; for instance $\langle \omega_{12} | \omega_{16} \rangle$ is 0.804 at I = 2 and 0.966 at I = 16. But as it turns out, after the full solution of Eq.(3) the low-spin part does not get affected much.

The lowest three eigenvalues are listed in Table II along with the corresponding g factor and the contributions from neutrons to total g and total spin I. The neutron spin $I_n = \langle \Psi_I | J_z^n | \Psi_I \rangle$ is a qualitative measure of the two quasineutron ($i_{13/2}$) alignment and in fact for each I the state with maximum I_n belongs to the s-band which can be seen in Fig.1. As discussed in I the proton contribution is purely collective and for every state the proton contribution to total g factor, $g_p = g - g_n$ can be almost entirely accounted for by I_p/I .

In Fig.1 the two dashed curves labelled g and s are the states projected simply from the CHF wavefunctions $|\omega_0\rangle$ and $|\omega_{16}\rangle$, respectively. They represent approximately the unperturbed g and s bands. Then the three sets of energies listed in Table II are plotted. The two solid curves are the g and s bands, whereas the dash-dot curve joining squares (■) and marked II represents some two quasineutron band having less alignment than the s band. Since our main interest is in the low spin part, there is no confusion between the s band and the curve II at least for I = 2 to 8. Beyond this we have essentially followed a smooth continuation. Also it is clear from Table II that for $I > 10$ the g band contains a sizeable amount of neutron alignment which is also reflected from the values of g factors. It would be interesting to see if the g factor measurements for the ground band states above the band crossing region support these features. This is obviously a consequence of the interaction of the g band with the s band in the higher spin region.

Thus, like in I, we find that the s band remains parabolic in shape with the energy minimum at around I = 8-10 though after diagonalization the levels I = 8-12 show some irregularity. We should add that in the past there have been some attempts, for example, by Rasmussen et al. [10] and Bengtsson and Frauendorf [11] to predict the low-spin part of the s band. From an empirical least squares fit to data and extrapolation Rasmussen et al. get the band head spin for the s band of ^{164}Er , $I_0 \approx 4$ to 6 units. On the other hand, extracting 'experimental quasiparticle levels' from N = 95, 97 neighbouring nuclei Bengtsson and Frauendorf get $I_0 = 6$ at which the cranking

frequency $\omega = 0$. In fact when Hamamoto [12] first pointed out the problems of the cranking model in the band crossing region, as a remedy, she had diagonalized the interaction Hamiltonian adding a term $(I - J_x)^2$ and there also she gets a parabolic shape (Fig.7 in Ref.12) for the s-band with a minimum at $I_0 \approx i$, where i is the magnitude of the aligned spin.

Recent experimental measurements for the isotones ^{164}Er [13] and ^{166}Yb [14] are extended down to 8^+ state of the s band whereas for ^{160}Dy [15] it is further lowered to $I_s = 4^+$. However, an important point to be noted is that so far in no case experimental observation has gone down to $I_s < i$. ^{160}Dy shows only an up bending whereas ^{164}Er and ^{166}Yb are good backbenders. Looking at the results of Almlager et al. [1] one can see that the excitation energy $E_8 - E_6$ (Fig.2) decreases if the Fermi surface goes down (better backbender) and the order of E_8 and E_6 may even get reversed. As far as our results for ^{158}Dy are concerned these are not to be taken quantitatively for this particular nucleus. These results are more appropriate for a good backbender as, without properly adjusting the interaction parameters, our yrast spectrum shows a sharp backbender.

We may conclude that even after properly orthogonalizing the angular momentum projected CHF states the E_I vs. I plot for the s band shows a parabolic behaviour with a minimum at I = 8-10 for the rare-earth backbending nuclei and g factors for very low spin states of the s-band assume large negative values ($g_2 \approx -1.5$) implying an anti-aligned configuration. We also predict a substantial reduction in the values of g factors for the ground band states above the band crossing region compared to the values for its low spin members. However, the effect of the variation of the shape parameters after the spin projection still remains to be seen.

ACKNOWLEDGMENTS

All the input data for the GCM calculation were generated during the stay of the authors at the Institut für Theoretische Physik, Giessen, and they feel extremely grateful to Prof. U. Mosel for the excellent computing facilities available there. The final version of the work has been completed at ICTP, Trieste, during a short visit of A.A. as an associate member of the Centre and he expresses his gratitude for the kind support.

REFERENCES

- [1] J. Almerger, I. Hamamoto, G. Leander and J.O. Rasmussen, Phys. Letts. 90B (1980) 1.
- [2] A. Ansari and E. Wüst, Phys. Lett. 143B (1984) 309.
- [3] K. Hara, A. Hayashi and P. Ring, Nucl. Phys. A385 (1982) 14.
- [4] E. Wüst, A. Ansari and U. Mosel, Nucl. Phys. A435 (1985) 477.
- [5] H.J. Mang, Phys. Repts. 18 (1975) 325.
- [6] A.L. Goodman, Adv. Nucl. Phys. 11 (1979) 263.
- [7] A. Ansari and S.C.K. Nair, Nucl. Phys. A217 (1973) 245.
- [8] J.L. Egido, Phys. Rev. C27 (1983) 453.
- [9] P. Ring and P. Schuck, The Nuclear Many-Body Problems (Springer-Verlag, 1980).
- [10] J.O. Rasmussen, M.W. Guidry, T.E. Ward, C. Castaneda, L.K. Peker, E. Leber and J.H. Hamilton, Nucl. Phys. A332 (1979) 82.
- [11] R. Bengtsson and S. Frauendorf, Nucl. Phys. A327 (1979) 139.
- [12] I. Hamamoto, Nucl. Phys. A271 (1976) 15.
- [13] C.A. Fields, K.H. Hicks, R.A. Ristinen, F.W.N. De Boer, L.K. Peker, R.J. Peterson and P.M. Walker, Nucl. Phys. A422 (1984) 215.
- [14] C.A. Fields, K.H. Hicks and R.J. Peterson, Nucl. Phys. A431 (1984) 473.
- [15] Jin Gen-Ming, J.D. Garrett, G. Løvholden, T.F. Thorsteinsen, J.C. Waddington and J. Rekstad, Phys. Rev. Lett. 46 (1981) 222.

Table I

Angular momentum projected overlaps for a few cranking wave functions
 $\langle \Psi_I(\omega_0) | \Psi_I(\omega_{I_x}) \rangle$ with $I_x = 0, 4, 8, 12$ and 16 .

$I \backslash I_x$	0	4	8	12	16
2	1.0	0.974	0.882	0.707	0.226
4	1.0	0.971	0.861	0.633	0.186
6	1.0	0.968	0.835	0.565	0.163
8	1.0	0.964	0.804	0.500	0.148
10	1.0	0.958	0.768	0.442	0.139
12	1.0	0.950	0.728	0.395	0.136
14	1.0	0.941	0.686	0.359	0.137
16	1.0	0.930	0.646	0.334	0.144

Table II

The lowest three eigenvalues and the corresponding ϵ , ϵ_n and I_n for $I = 2$ to 16.

I	E_I [MeV]	ϵ	ϵ_n	I_n
2	-275.122	0.358	-0.025	1.27
	-272.510	-0.236	-0.209	2.09
	-271.501	-1.562	-0.625	3.85
4	-274.732	0.334	-0.031	2.62
	-272.427	-0.128	-0.171	3.87
	-271.967	-0.673	-0.343	5.32
6	-274.197	0.299	-0.040	4.08
	-272.423	-0.318	-0.226	6.57
	-271.952	-0.034	-0.145	5.41
8	-273.601	0.244	-0.056	5.77
	-272.589	-0.233	-0.198	8.32
	-271.517	0.161	-0.084	6.14
10	-273.074	0.112	-0.093	8.11
	-272.549	-0.047	-0.142	9.15
	-270.896	0.242	-0.059	7.11
12	-272.761	-0.079	-0.127	10.69
	-272.057	0.119	-0.093	9.65
	-269.886	0.289	-0.044	8.15
14	-272.445	0.0003	-0.124	12.39
	-271.450	0.151	-0.083	10.97
	-268.945	0.316	-0.035	9.26
16	-272.002	0.030	-0.115	13.83
	-270.761	0.160	-0.080	12.44
	-267.887	0.329	-0.031	10.44

The ground state energy $E_{I=0} = -275.302$ MeV.

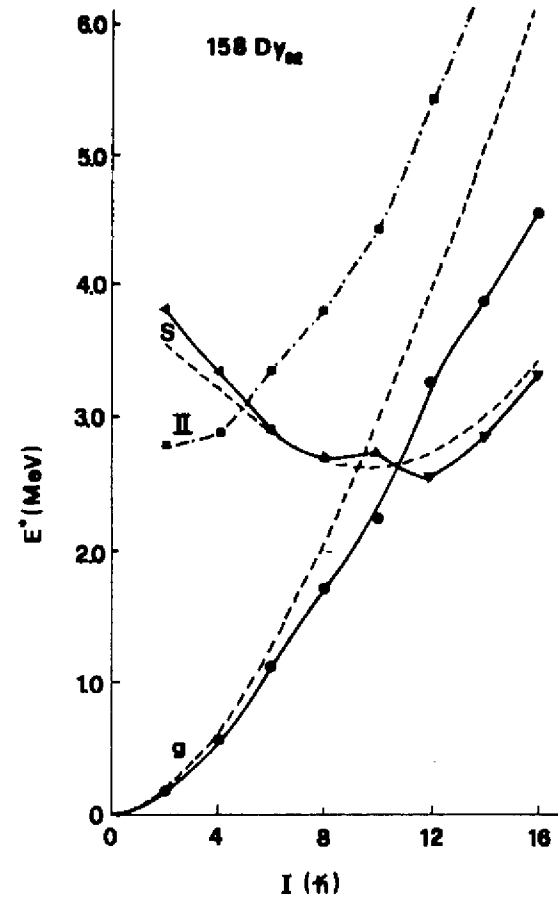


Fig.1

Excitation energy vs. spin plot for the ground and s bands. The dashed curves labelled g and s correspond to angular momentum projected states from the CHF states $|\omega = 0\rangle$ and $|\omega_I = 16\rangle$, respectively. Solid curves and the one marked II correspond to the GCM calculation.